

Atmospheric deposition of Heavy Metals on the Baltic Sea

HELCOM Baltic Sea Environment Fact Sheet (BSEFS), 2020

Authors: Ilia Ilyin, Oleg Travnikov, Olga Rozovskaya, Alexey Gusev, EMEP MSC-E

Key message

Levels of annual total atmospheric deposition of heavy metals to the Baltic Sea have decreased in period from 1990 to 2018 by 73% for cadmium and 35% for mercury, although the decrease was higher during the first half of the assessment period.

Results and Assessment

Relevance of the BSEFS for describing developments in the environment

This BSEFS shows the levels and trends in cadmium and mercury atmospheric deposition to the Baltic Sea. The deposition of heavy metals (HM) represents the pressure of the emission sources on the Baltic Sea aquatic environment as described in the BSEFS “Atmospheric emissions of heavy metals in the Baltic Sea region”.

Policy relevance and policy reference

The Baltic Sea Action Plan states the ecological objectives that concentrations of hazardous substances in the environment are to be close to background values for naturally occurring substances. HELCOM Recommendation 31E/1 identifies the list of regional priority substances for the Baltic Sea.

The relevant policy to the control of emissions of heavy metals to the atmosphere on European scale is set in the framework of UN ECE Convention on Long-Range Transboundary Air Pollution (CLRTAP). The CLRTAP Protocol on Heavy Metals (1998) targets three particularly harmful metals: lead, cadmium and mercury. According to one of the basic obligations, the emissions of these three metals must be reduced below the emission levels in 1990. In addition, specific requirements and measures on reduction of mercury emissions are given in the UNEP 2013 Minamata Convention.

For EU member states the policy frame is set by the EU IED Directive, whereas for the Russian Federation the corresponding policy framework is embraced by the Russian Federal Act on the environmental protection and the Act on protection of atmospheric air.

Assessment

Airborne input of heavy metals to the Baltic Sea has substantially decreased in the period from 1990 to 2018. Results of model simulations based on the officially reported EMEP emission data indicate that levels of annual total atmospheric deposition of heavy metals to the Baltic Sea have decreased in the period from 1990 to 2018 by 73% for cadmium and 35% for mercury (Figure 1). The most substantial decrease of cadmium is noted for the Sound and the Gulf of Riga sub-basins (78% each). For mercury, the highest reduction occurred in the Sound sub-basin (60%). The highest level of cadmium deposition fluxes over the Baltic Sea in 2018 is noted for the Sound and the Kattegat sub-basins (Figure 2). In case of mercury the

highest flux in 2018 takes place in Bothnian Bay followed by the Sound sub-basin (Figure 3). The HELCOM Contracting Parties contributed to cadmium and mercury deposition over the Baltic Sea in 2018 about 39% and 15%, respectively, with the largest contributions made by Poland and Germany. Reduction of atmospheric input of cadmium and mercury to the Baltic Sea is a result of various activities including abatement measures, economic contraction, and industrial restructuring, which took place in the HELCOM countries as well as other EMEP countries.

Presented model estimates of Cd and Hg total deposition differ from previously published modelling results [Gauss et al., 2019]. Comparison of current and previous model estimates is discussed in the report [Guass et al., 2020].

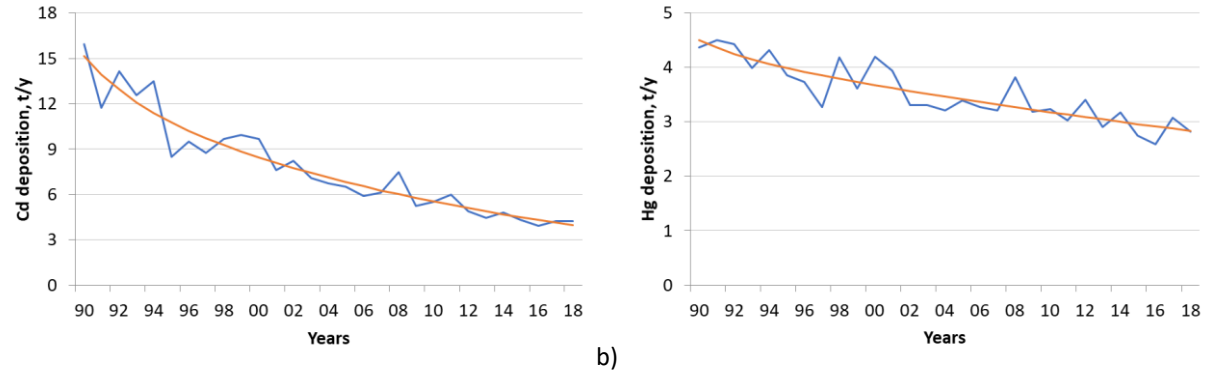


Figure 1. Changes of modelled (blue line) and normalized (red line) total annual atmospheric deposition of cadmium (a) and mercury (b) to the Baltic Sea for the period 1990-2018, (t/y).

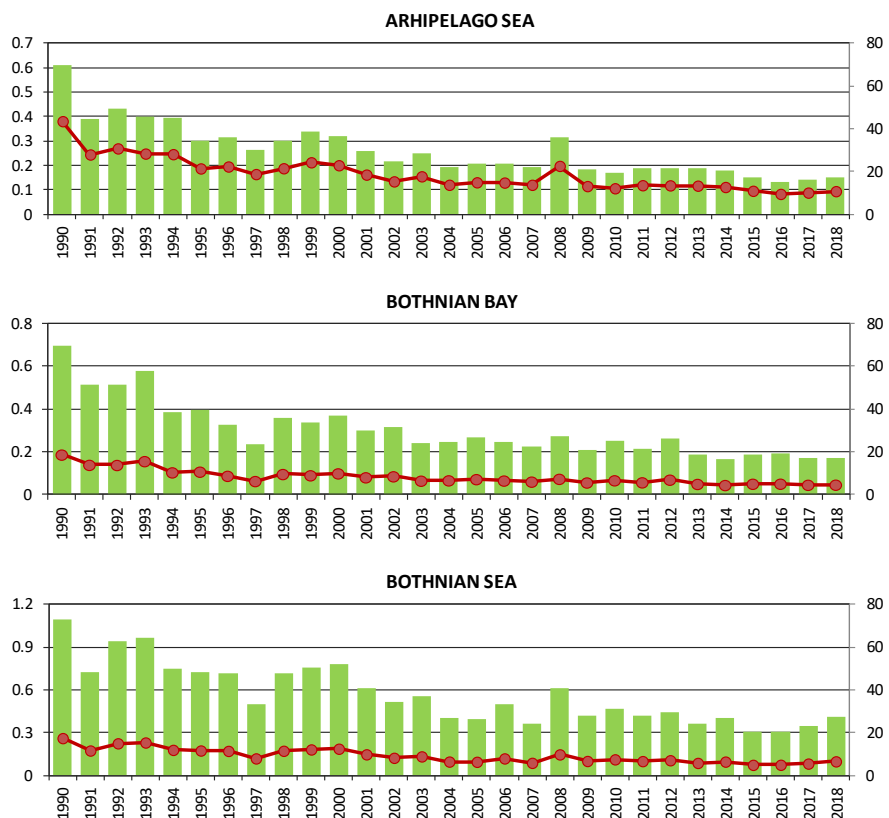


Figure 2. Time-series of computed total annual atmospheric deposition of cadmium to nine sub-basins of the Baltic Sea for the period 1990-2018 in tonnes/year as bars (left axis) and total deposition fluxes in g/km²/year as lines (right axis).

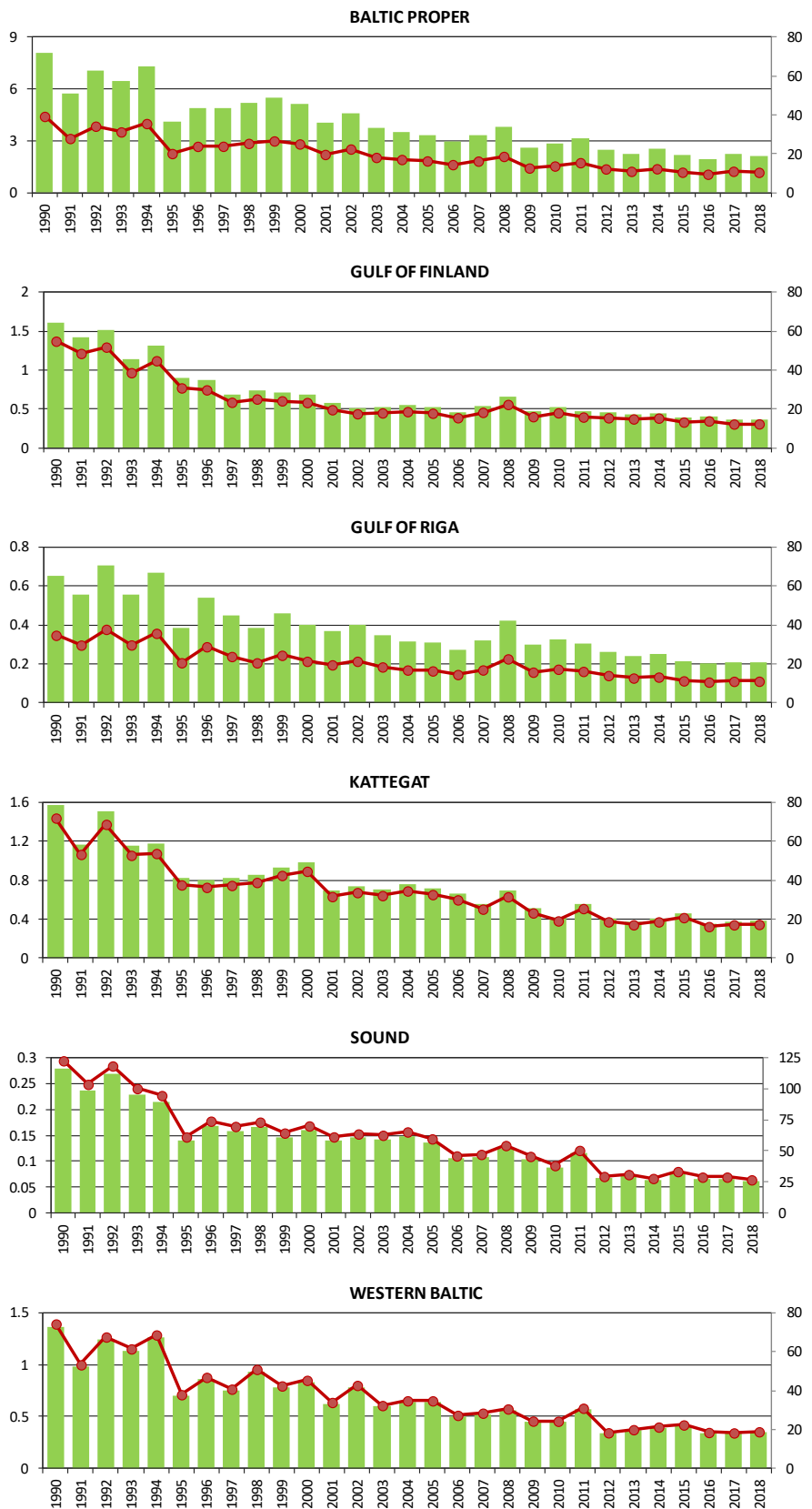


Figure 2 (continued). Time-series of computed total annual atmospheric deposition of cadmium to nine sub-basins of the Baltic Sea for the period 1990–2018 in tonnes/year as bars (left axis) and total deposition fluxes in g/km²/year as lines (right axis).

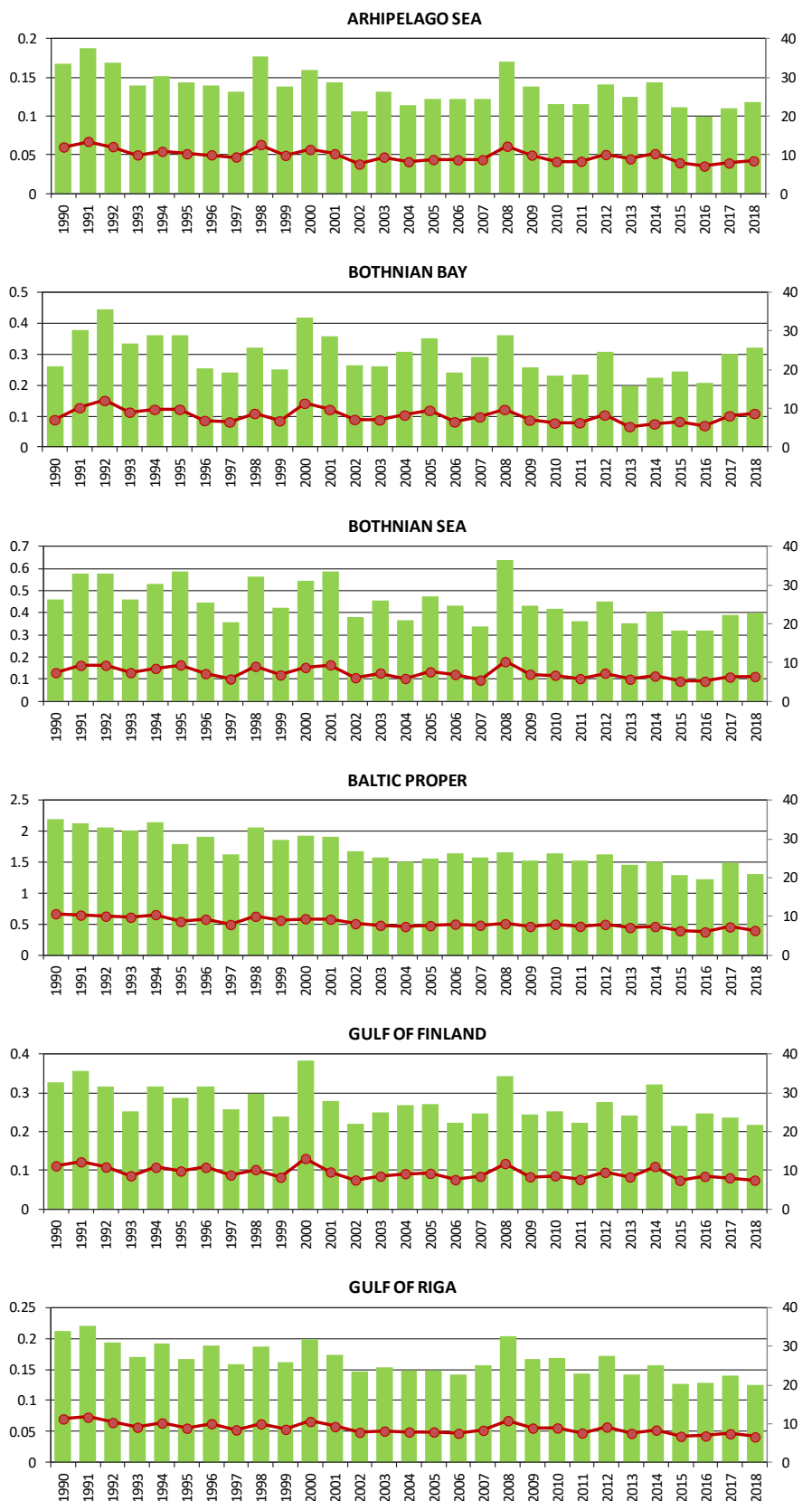


Figure 3. Time-series of computed total annual atmospheric deposition of mercury to nine sub-basins of the Baltic Sea for the period 1990–2018 in tonnes/year as bars (left axis) and total deposition fluxes in g/km²/year as lines (right axis).

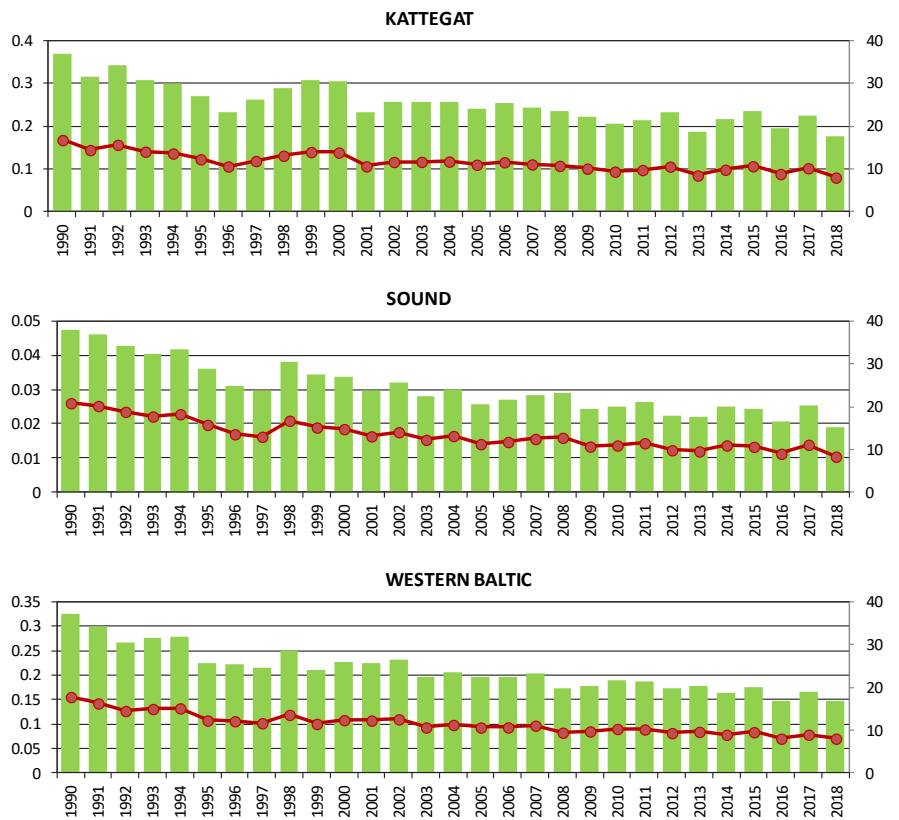


Figure 3 (continued). Time-series of computed total annual atmospheric deposition of mercury to nine sub-basins of the Baltic Sea for the period 1990-2018 in tonnes/year as bars (left axis) and total deposition fluxes in g/km²/year as lines (right axis).

Data

Numerical data on computed HM depositions to the Baltic Sea are given in the following tables.

Table 1. Computed total annual deposition of cadmium to nine Baltic Sea sub-basins, the whole Baltic Sea (BAS) and normalized deposition to the Baltic Sea (Norm) for the period 1990-2018. Units: tonnes/year.

| | ARC | BOB | BOS | BAP | GUF | GUR | KAT | SOU | WEB | BAS | Norm |
|------|------------|------------|------------|------------|------------|------------|------------|------------|------------|------------|-------------|
| 1990 | 0.610 | 0.693 | 1.090 | 8.068 | 1.609 | 0.650 | 1.576 | 0.279 | 1.364 | 15.94 | 15.17 |
| 1991 | 0.391 | 0.516 | 0.726 | 5.725 | 1.424 | 0.556 | 1.167 | 0.236 | 0.979 | 11.72 | 13.95 |
| 1992 | 0.431 | 0.514 | 0.937 | 7.030 | 1.520 | 0.707 | 1.505 | 0.269 | 1.241 | 14.16 | 12.95 |
| 1993 | 0.397 | 0.580 | 0.961 | 6.422 | 1.134 | 0.557 | 1.157 | 0.228 | 1.129 | 12.56 | 12.11 |
| 1994 | 0.393 | 0.386 | 0.745 | 7.309 | 1.314 | 0.669 | 1.178 | 0.215 | 1.260 | 13.47 | 11.40 |
| 1995 | 0.300 | 0.398 | 0.726 | 4.130 | 0.904 | 0.387 | 0.824 | 0.140 | 0.697 | 8.51 | 10.77 |
| 1996 | 0.312 | 0.326 | 0.715 | 4.894 | 0.874 | 0.540 | 0.797 | 0.168 | 0.860 | 9.49 | 10.22 |
| 1997 | 0.263 | 0.236 | 0.495 | 4.900 | 0.686 | 0.446 | 0.818 | 0.159 | 0.749 | 8.75 | 9.73 |
| 1998 | 0.301 | 0.357 | 0.718 | 5.204 | 0.736 | 0.386 | 0.852 | 0.167 | 0.935 | 9.66 | 9.27 |
| 1999 | 0.340 | 0.336 | 0.758 | 5.464 | 0.708 | 0.458 | 0.931 | 0.147 | 0.780 | 9.92 | 8.86 |
| 2000 | 0.321 | 0.369 | 0.779 | 5.144 | 0.682 | 0.400 | 0.978 | 0.160 | 0.832 | 9.66 | 8.47 |
| 2001 | 0.259 | 0.301 | 0.614 | 4.033 | 0.574 | 0.366 | 0.693 | 0.140 | 0.624 | 7.60 | 8.10 |
| 2002 | 0.215 | 0.318 | 0.513 | 4.607 | 0.513 | 0.400 | 0.738 | 0.145 | 0.785 | 8.23 | 7.76 |
| 2003 | 0.248 | 0.242 | 0.554 | 3.720 | 0.526 | 0.346 | 0.704 | 0.143 | 0.595 | 7.08 | 7.43 |
| 2004 | 0.192 | 0.248 | 0.402 | 3.499 | 0.545 | 0.317 | 0.757 | 0.149 | 0.639 | 6.75 | 7.12 |
| 2005 | 0.209 | 0.269 | 0.396 | 3.346 | 0.521 | 0.308 | 0.715 | 0.136 | 0.639 | 6.54 | 6.83 |
| 2006 | 0.207 | 0.244 | 0.495 | 2.957 | 0.453 | 0.273 | 0.656 | 0.105 | 0.502 | 5.89 | 6.55 |
| 2007 | 0.192 | 0.226 | 0.365 | 3.328 | 0.534 | 0.317 | 0.552 | 0.108 | 0.523 | 6.14 | 6.28 |
| 2008 | 0.316 | 0.274 | 0.613 | 3.827 | 0.654 | 0.424 | 0.691 | 0.124 | 0.563 | 7.48 | 6.02 |
| 2009 | 0.184 | 0.211 | 0.420 | 2.594 | 0.469 | 0.296 | 0.509 | 0.104 | 0.448 | 5.23 | 5.78 |
| 2010 | 0.170 | 0.249 | 0.468 | 2.809 | 0.527 | 0.324 | 0.420 | 0.087 | 0.447 | 5.50 | 5.54 |
| 2011 | 0.190 | 0.214 | 0.416 | 3.161 | 0.463 | 0.303 | 0.558 | 0.115 | 0.569 | 5.99 | 5.32 |
| 2012 | 0.189 | 0.260 | 0.442 | 2.497 | 0.452 | 0.263 | 0.409 | 0.067 | 0.338 | 4.92 | 5.10 |
| 2013 | 0.187 | 0.186 | 0.363 | 2.243 | 0.435 | 0.239 | 0.376 | 0.071 | 0.367 | 4.47 | 4.89 |
| 2014 | 0.178 | 0.167 | 0.402 | 2.517 | 0.448 | 0.249 | 0.409 | 0.064 | 0.392 | 4.82 | 4.70 |
| 2015 | 0.153 | 0.189 | 0.307 | 2.149 | 0.388 | 0.212 | 0.456 | 0.076 | 0.412 | 4.34 | 4.50 |
| 2016 | 0.133 | 0.190 | 0.309 | 1.936 | 0.405 | 0.201 | 0.356 | 0.066 | 0.341 | 3.94 | 4.32 |
| 2017 | 0.141 | 0.171 | 0.344 | 2.249 | 0.358 | 0.208 | 0.375 | 0.066 | 0.337 | 4.25 | 4.15 |
| 2018 | 0.151 | 0.173 | 0.409 | 2.136 | 0.360 | 0.209 | 0.379 | 0.061 | 0.348 | 4.23 | 3.98 |

Table 2. Computed annual total deposition of mercury to nine Baltic Sea sub-basins, the whole Baltic Sea (BAS) and normalized deposition to the Baltic Sea (Norm) for the period 1990-2017. Units: tonnes/year.

| | ARC | BOB | BOS | BAP | GUF | GUR | KAT | SOU | WEB | BAS | Norm |
|------|------------|------------|------------|------------|------------|------------|------------|------------|------------|------------|-------------|
| 1990 | 0.168 | 0.262 | 0.460 | 2.196 | 0.327 | 0.211 | 0.368 | 0.047 | 0.326 | 4.37 | 4.50 |
| 1991 | 0.188 | 0.377 | 0.578 | 2.120 | 0.356 | 0.220 | 0.316 | 0.046 | 0.299 | 4.50 | 4.36 |
| 1992 | 0.169 | 0.446 | 0.579 | 2.066 | 0.317 | 0.194 | 0.343 | 0.043 | 0.266 | 4.42 | 4.24 |
| 1993 | 0.139 | 0.334 | 0.460 | 2.009 | 0.251 | 0.171 | 0.308 | 0.040 | 0.275 | 3.99 | 4.14 |
| 1994 | 0.152 | 0.361 | 0.528 | 2.150 | 0.315 | 0.192 | 0.299 | 0.042 | 0.278 | 4.32 | 4.06 |
| 1995 | 0.143 | 0.361 | 0.584 | 1.783 | 0.287 | 0.166 | 0.269 | 0.036 | 0.225 | 3.86 | 3.98 |
| 1996 | 0.139 | 0.255 | 0.444 | 1.903 | 0.315 | 0.189 | 0.233 | 0.031 | 0.222 | 3.73 | 3.91 |
| 1997 | 0.132 | 0.241 | 0.357 | 1.619 | 0.257 | 0.159 | 0.260 | 0.030 | 0.214 | 3.27 | 3.85 |
| 1998 | 0.177 | 0.322 | 0.562 | 2.058 | 0.298 | 0.187 | 0.288 | 0.038 | 0.250 | 4.18 | 3.79 |
| 1999 | 0.137 | 0.252 | 0.422 | 1.850 | 0.240 | 0.161 | 0.306 | 0.035 | 0.211 | 3.61 | 3.73 |
| 2000 | 0.159 | 0.419 | 0.544 | 1.929 | 0.382 | 0.199 | 0.304 | 0.034 | 0.227 | 4.20 | 3.67 |
| 2001 | 0.144 | 0.359 | 0.586 | 1.902 | 0.280 | 0.174 | 0.233 | 0.030 | 0.225 | 3.93 | 3.62 |
| 2002 | 0.106 | 0.265 | 0.378 | 1.668 | 0.219 | 0.146 | 0.256 | 0.032 | 0.231 | 3.30 | 3.57 |
| 2003 | 0.131 | 0.260 | 0.453 | 1.577 | 0.248 | 0.153 | 0.256 | 0.028 | 0.196 | 3.30 | 3.51 |
| 2004 | 0.115 | 0.307 | 0.365 | 1.512 | 0.267 | 0.148 | 0.258 | 0.030 | 0.207 | 3.21 | 3.46 |
| 2005 | 0.122 | 0.352 | 0.473 | 1.562 | 0.269 | 0.148 | 0.241 | 0.026 | 0.195 | 3.39 | 3.41 |
| 2006 | 0.121 | 0.242 | 0.431 | 1.640 | 0.221 | 0.142 | 0.254 | 0.027 | 0.196 | 3.27 | 3.37 |
| 2007 | 0.122 | 0.289 | 0.339 | 1.579 | 0.247 | 0.156 | 0.243 | 0.028 | 0.203 | 3.21 | 3.32 |
| 2008 | 0.171 | 0.360 | 0.638 | 1.664 | 0.344 | 0.203 | 0.236 | 0.029 | 0.173 | 3.82 | 3.27 |
| 2009 | 0.139 | 0.258 | 0.434 | 1.516 | 0.243 | 0.167 | 0.221 | 0.024 | 0.179 | 3.18 | 3.22 |
| 2010 | 0.115 | 0.230 | 0.418 | 1.634 | 0.251 | 0.168 | 0.206 | 0.025 | 0.189 | 3.24 | 3.18 |
| 2011 | 0.116 | 0.233 | 0.363 | 1.525 | 0.222 | 0.143 | 0.214 | 0.026 | 0.187 | 3.03 | 3.13 |
| 2012 | 0.141 | 0.307 | 0.451 | 1.626 | 0.277 | 0.172 | 0.232 | 0.022 | 0.172 | 3.40 | 3.09 |
| 2013 | 0.125 | 0.197 | 0.354 | 1.464 | 0.242 | 0.142 | 0.186 | 0.022 | 0.177 | 2.91 | 3.04 |
| 2014 | 0.144 | 0.223 | 0.405 | 1.515 | 0.322 | 0.158 | 0.216 | 0.025 | 0.164 | 3.17 | 3.00 |
| 2015 | 0.111 | 0.245 | 0.321 | 1.288 | 0.216 | 0.127 | 0.234 | 0.024 | 0.175 | 2.74 | 2.96 |
| 2016 | 0.099 | 0.206 | 0.319 | 1.226 | 0.246 | 0.129 | 0.194 | 0.021 | 0.148 | 2.59 | 2.92 |
| 2017 | 0.110 | 0.299 | 0.388 | 1.494 | 0.235 | 0.140 | 0.223 | 0.025 | 0.165 | 3.08 | 2.88 |
| 2018 | 0.118 | 0.322 | 0.397 | 1.303 | 0.217 | 0.125 | 0.176 | 0.019 | 0.148 | 2.82 | 2.83 |

Table 3. Computed contributions by country to annual total deposition of cadmium to nine Baltic Sea sub-basins for the year 2018. Units: tonnes/year. HELCOM: contribution of anthropogenic sources of HELCOM countries; EMEP: contribution of anthropogenic sources in other EMEP countries; NSR: contributions of sources other than primary anthropogenic emissions (natural, secondary (re-suspension), and non-EMEP sources).

| Country | ARC | BOB | BOS | BAP | GUF | GUR | KAT | SOU | WEB | BAS |
|--------------|---------|---------|---------|---------|---------|---------|---------|---------|---------|---------|
| DK | 1.2E-03 | 6.4E-04 | 2.2E-03 | 3.7E-02 | 1.3E-03 | 1.2E-03 | 4.4E-02 | 7.8E-03 | 3.7E-02 | 1.3E-01 |
| EE | 4.5E-03 | 3.4E-03 | 7.8E-03 | 2.1E-02 | 5.6E-02 | 9.7E-03 | 3.7E-04 | 4.7E-05 | 4.5E-04 | 1.0E-01 |
| FI | 1.2E-02 | 2.4E-02 | 2.1E-02 | 1.3E-02 | 3.3E-02 | 2.5E-03 | 2.6E-04 | 2.9E-05 | 3.0E-04 | 1.1E-01 |
| DE | 7.7E-03 | 8.0E-03 | 1.8E-02 | 2.3E-01 | 9.6E-03 | 1.2E-02 | 5.3E-02 | 6.2E-03 | 8.0E-02 | 4.2E-01 |
| LV | 3.9E-03 | 1.3E-03 | 5.2E-03 | 3.5E-02 | 6.4E-03 | 2.7E-02 | 6.3E-04 | 1.0E-04 | 7.5E-04 | 8.0E-02 |
| LT | 1.1E-03 | 4.3E-04 | 1.7E-03 | 1.3E-02 | 1.2E-03 | 3.1E-03 | 2.9E-04 | 5.2E-05 | 3.7E-04 | 2.2E-02 |
| PL | 1.4E-02 | 1.0E-02 | 3.2E-02 | 3.2E-01 | 1.5E-02 | 2.2E-02 | 1.9E-02 | 2.8E-03 | 1.4E-02 | 4.5E-01 |
| RU | 1.2E-02 | 1.8E-02 | 4.0E-02 | 1.2E-01 | 7.3E-02 | 1.6E-02 | 3.7E-03 | 4.5E-04 | 4.1E-03 | 2.8E-01 |
| SE | 2.9E-03 | 1.2E-02 | 1.3E-02 | 2.5E-02 | 1.9E-03 | 1.5E-03 | 3.8E-03 | 4.8E-04 | 9.7E-04 | 6.2E-02 |
| AF | 2.1E-04 | 3.1E-04 | 6.1E-04 | 3.6E-03 | 5.5E-04 | 4.6E-04 | 4.2E-04 | 3.5E-05 | 4.0E-04 | 6.6E-03 |
| AL | 2.1E-05 | 2.8E-05 | 6.7E-05 | 3.7E-04 | 4.1E-05 | 4.0E-05 | 3.7E-05 | 3.5E-06 | 3.1E-05 | 6.4E-04 |
| AM | 4.7E-07 | 7.3E-07 | 2.1E-06 | 4.9E-06 | 1.3E-06 | 4.8E-07 | 2.2E-07 | 2.3E-08 | 1.3E-07 | 1.0E-05 |
| AS | 6.4E-05 | 9.3E-05 | 2.7E-04 | 6.4E-04 | 1.6E-04 | 6.8E-05 | 2.2E-05 | 2.1E-06 | 1.7E-05 | 1.3E-03 |
| AT | 5.0E-04 | 4.4E-04 | 1.3E-03 | 1.3E-02 | 7.4E-04 | 1.1E-03 | 1.8E-03 | 2.4E-04 | 1.2E-03 | 2.0E-02 |
| AZ | 3.6E-06 | 6.0E-06 | 1.6E-05 | 3.5E-05 | 9.1E-06 | 4.5E-06 | 1.4E-06 | 1.3E-07 | 1.3E-06 | 7.7E-05 |
| BA | 5.1E-04 | 3.8E-04 | 1.1E-03 | 6.4E-03 | 7.3E-04 | 6.9E-04 | 4.9E-04 | 4.7E-05 | 3.6E-04 | 1.1E-02 |
| BE | 4.5E-04 | 4.2E-04 | 1.1E-03 | 1.2E-02 | 5.4E-04 | 6.6E-04 | 3.9E-03 | 3.8E-04 | 4.1E-03 | 2.4E-02 |
| BG | 2.3E-04 | 4.8E-04 | 1.0E-03 | 3.5E-03 | 6.0E-04 | 4.1E-04 | 3.1E-04 | 3.0E-05 | 2.5E-04 | 6.9E-03 |
| BY | 1.2E-03 | 6.8E-04 | 2.3E-03 | 1.2E-02 | 2.2E-03 | 2.5E-03 | 3.9E-04 | 6.1E-05 | 5.1E-04 | 2.2E-02 |
| CH | 2.9E-04 | 3.8E-04 | 7.9E-04 | 7.1E-03 | 3.9E-04 | 5.0E-04 | 1.3E-03 | 1.5E-04 | 1.4E-03 | 1.2E-02 |
| CY | 3.4E-07 | 7.9E-07 | 1.5E-06 | 2.5E-06 | 9.5E-07 | 4.5E-07 | 1.7E-07 | 1.4E-08 | 1.5E-07 | 6.9E-06 |
| CZ | 1.1E-03 | 9.3E-04 | 2.7E-03 | 2.8E-02 | 1.4E-03 | 2.1E-03 | 3.5E-03 | 4.6E-04 | 2.6E-03 | 4.3E-02 |
| ES | 2.2E-04 | 4.6E-04 | 7.3E-04 | 3.9E-03 | 2.8E-04 | 2.6E-04 | 1.1E-03 | 9.6E-05 | 9.4E-04 | 8.0E-03 |
| FR | 4.6E-04 | 5.7E-04 | 1.1E-03 | 9.7E-03 | 5.9E-04 | 5.7E-04 | 3.0E-03 | 2.8E-04 | 2.9E-03 | 1.9E-02 |
| GB | 1.8E-03 | 1.5E-03 | 3.7E-03 | 3.1E-02 | 2.3E-03 | 2.0E-03 | 1.1E-02 | 9.9E-04 | 8.5E-03 | 6.3E-02 |
| GE | 1.0E-05 | 2.0E-05 | 4.6E-05 | 1.0E-04 | 3.5E-05 | 1.2E-05 | 5.5E-06 | 5.6E-07 | 3.8E-06 | 2.4E-04 |
| GR | 1.0E-04 | 2.5E-04 | 5.5E-04 | 1.7E-03 | 3.0E-04 | 2.0E-04 | 1.8E-04 | 1.7E-05 | 1.4E-04 | 3.5E-03 |
| HR | 2.8E-04 | 2.1E-04 | 7.4E-04 | 4.7E-03 | 3.8E-04 | 4.9E-04 | 3.0E-04 | 4.0E-05 | 1.7E-04 | 7.3E-03 |
| HU | 7.1E-04 | 5.7E-04 | 1.9E-03 | 1.2E-02 | 9.6E-04 | 1.2E-03 | 1.0E-03 | 1.3E-04 | 5.8E-04 | 1.9E-02 |
| IE | 6.3E-05 | 8.1E-05 | 1.4E-04 | 1.0E-03 | 7.9E-05 | 6.0E-05 | 3.9E-04 | 3.5E-05 | 2.7E-04 | 2.2E-03 |
| IS | 1.8E-07 | 4.3E-07 | 4.5E-07 | 2.1E-06 | 2.9E-07 | 2.2E-07 | 5.3E-07 | 4.4E-08 | 3.2E-07 | 4.6E-06 |
| IT | 4.6E-04 | 4.2E-04 | 1.2E-03 | 8.6E-03 | 9.3E-04 | 8.9E-04 | 6.7E-04 | 8.6E-05 | 5.6E-04 | 1.4E-02 |
| KY | 4.8E-06 | 5.2E-06 | 1.5E-05 | 4.3E-05 | 1.0E-05 | 4.2E-06 | 1.3E-06 | 1.5E-07 | 7.8E-07 | 8.5E-05 |
| KZ | 2.1E-04 | 2.6E-04 | 7.9E-04 | 1.6E-03 | 4.6E-04 | 2.2E-04 | 4.8E-05 | 4.9E-06 | 2.8E-05 | 3.6E-03 |
| LI | 9.4E-07 | 1.1E-06 | 2.4E-06 | 2.4E-05 | 1.3E-06 | 1.7E-06 | 4.6E-06 | 5.2E-07 | 4.6E-06 | 4.1E-05 |
| LU | 1.9E-05 | 2.6E-05 | 4.6E-05 | 4.6E-04 | 2.5E-05 | 2.3E-05 | 1.3E-04 | 1.3E-05 | 1.6E-04 | 9.0E-04 |
| MC | 5.8E-08 | 6.2E-08 | 1.7E-07 | 8.1E-07 | 9.4E-08 | 7.9E-08 | 1.4E-07 | 1.7E-08 | 1.1E-07 | 1.5E-06 |
| MD | 2.1E-04 | 1.9E-04 | 5.0E-04 | 1.8E-03 | 3.4E-04 | 2.5E-04 | 7.0E-05 | 1.3E-05 | 1.2E-04 | 3.5E-03 |
| ME | 3.8E-05 | 3.3E-05 | 9.1E-05 | 5.5E-04 | 6.5E-05 | 5.9E-05 | 5.6E-05 | 5.8E-06 | 3.9E-05 | 9.4E-04 |
| MK | 6.4E-05 | 1.3E-04 | 2.8E-04 | 1.4E-03 | 1.8E-04 | 1.5E-04 | 1.9E-04 | 2.0E-05 | 1.3E-04 | 2.6E-03 |
| MT | 1.2E-07 | 2.2E-07 | 4.6E-07 | 3.4E-06 | 4.1E-07 | 3.9E-07 | 1.7E-07 | 1.4E-08 | 2.1E-07 | 5.4E-06 |
| NL | 1.3E-03 | 1.1E-03 | 3.1E-03 | 3.3E-02 | 1.7E-03 | 2.1E-03 | 1.1E-02 | 1.1E-03 | 1.2E-02 | 6.5E-02 |
| NO | 5.1E-04 | 8.2E-04 | 1.5E-03 | 3.6E-03 | 5.1E-04 | 3.4E-04 | 1.2E-03 | 5.8E-05 | 3.5E-04 | 8.8E-03 |
| PT | 2.6E-05 | 7.0E-05 | 8.7E-05 | 6.5E-04 | 3.7E-05 | 2.9E-05 | 1.6E-04 | 1.4E-05 | 1.3E-04 | 1.2E-03 |
| RO | 1.4E-03 | 1.5E-03 | 3.9E-03 | 1.5E-02 | 2.3E-03 | 1.5E-03 | 9.1E-04 | 1.2E-04 | 8.5E-04 | 2.7E-02 |
| RS | 1.1E-03 | 7.9E-04 | 2.5E-03 | 1.5E-02 | 1.5E-03 | 1.3E-03 | 1.3E-03 | 1.3E-04 | 8.7E-04 | 2.5E-02 |
| SI | 1.9E-04 | 1.6E-04 | 5.7E-04 | 3.7E-03 | 2.7E-04 | 3.7E-04 | 2.8E-04 | 4.2E-05 | 1.5E-04 | 5.7E-03 |
| SK | 1.1E-03 | 9.0E-04 | 2.8E-03 | 2.2E-02 | 1.6E-03 | 2.1E-03 | 1.9E-03 | 2.8E-04 | 1.1E-03 | 3.4E-02 |
| TJ | 3.1E-06 | 2.9E-06 | 9.1E-06 | 2.9E-05 | 5.0E-06 | 2.5E-06 | 9.4E-07 | 1.1E-07 | 4.4E-07 | 5.3E-05 |
| TM | 8.1E-06 | 1.2E-05 | 4.2E-05 | 9.1E-05 | 1.8E-05 | 9.8E-06 | 2.9E-06 | 2.6E-07 | 2.1E-06 | 1.9E-04 |
| TR | 5.8E-04 | 1.4E-03 | 2.9E-03 | 5.9E-03 | 2.6E-03 | 1.4E-03 | 2.7E-04 | 2.5E-05 | 2.1E-04 | 1.5E-02 |
| UA | 8.2E-04 | 8.4E-04 | 2.5E-03 | 5.0E-03 | 2.1E-03 | 1.2E-03 | 2.5E-04 | 2.5E-05 | 2.1E-04 | 1.3E-02 |
| UZ | 3.4E-05 | 3.8E-05 | 1.2E-04 | 3.5E-04 | 7.0E-05 | 3.1E-05 | 1.1E-05 | 1.1E-06 | 6.9E-06 | 6.6E-04 |
| NSR | 0.075 | 0.080 | 0.224 | 1.059 | 0.133 | 0.091 | 0.211 | 0.039 | 0.170 | 2.082 |
| EMEP | 0.016 | 0.017 | 0.043 | 0.269 | 0.027 | 0.025 | 0.048 | 0.005 | 0.041 | 0.491 |
| HELCOM | 0.060 | 0.078 | 0.141 | 0.809 | 0.198 | 0.095 | 0.125 | 0.018 | 0.139 | 1.662 |
| Total | 0.151 | 0.174 | 0.408 | 2.138 | 0.358 | 0.211 | 0.383 | 0.062 | 0.349 | 4.235 |

Table 4. Computed contributions by country to annual total deposition of mercury to nine Baltic Sea sub-basins for the year 2018. Units: tonnes/year. HELCOM: contribution of anthropogenic sources of HELCOM countries; EMEP: contribution of anthropogenic sources in other EMEP countries; NSR: contributions of sources other than primary anthropogenic emissions (natural, secondary (re-suspension), and non-EMEP sources).

| Country | ARC | BOB | BOS | BAP | GUF | GUR | KAT | SOU | WEB | BAS |
|---------------|---------|---------|---------|---------|---------|---------|---------|---------|---------|---------|
| DK | 1.7E-04 | 2.8E-04 | 6.4E-04 | 1.1E-02 | 2.6E-04 | 2.7E-04 | 5.1E-03 | 5.7E-04 | 2.4E-03 | 2.0E-02 |
| EE | 4.2E-04 | 8.9E-04 | 1.6E-03 | 4.2E-03 | 1.5E-02 | 8.8E-04 | 7.7E-05 | 2.9E-06 | 2.3E-05 | 2.3E-02 |
| FI | 8.7E-04 | 5.9E-03 | 2.6E-03 | 1.5E-03 | 2.9E-03 | 1.9E-04 | 2.4E-05 | 1.1E-06 | 9.4E-06 | 1.4E-02 |
| DE | 2.1E-03 | 3.5E-03 | 8.4E-03 | 9.1E-02 | 3.1E-03 | 3.8E-03 | 1.0E-02 | 8.4E-04 | 9.7E-03 | 1.3E-01 |
| LV | 6.2E-05 | 4.6E-05 | 1.6E-04 | 1.1E-03 | 2.3E-04 | 8.5E-04 | 2.4E-05 | 1.4E-06 | 7.1E-06 | 2.5E-03 |
| LT | 4.2E-05 | 3.2E-05 | 1.0E-04 | 1.2E-03 | 9.6E-05 | 2.8E-04 | 2.4E-05 | 1.8E-06 | 7.1E-06 | 1.7E-03 |
| PL | 3.8E-03 | 4.7E-03 | 1.4E-02 | 1.2E-01 | 4.8E-03 | 6.9E-03 | 4.3E-03 | 3.1E-04 | 1.8E-03 | 1.6E-01 |
| RU | 4.0E-04 | 2.1E-03 | 1.9E-03 | 8.6E-03 | 2.3E-03 | 9.1E-04 | 2.3E-04 | 1.8E-05 | 8.9E-05 | 1.7E-02 |
| SE | 3.6E-04 | 2.6E-03 | 2.3E-03 | 3.7E-03 | 2.6E-04 | 2.0E-04 | 8.3E-04 | 3.7E-05 | 6.6E-05 | 1.0E-02 |
| AF | 6.3E-05 | 1.6E-04 | 2.1E-04 | 8.5E-04 | 1.5E-04 | 1.0E-04 | 1.2E-04 | 9.1E-06 | 9.9E-05 | 1.8E-03 |
| AL | 4.1E-06 | 1.0E-05 | 1.3E-05 | 5.8E-05 | 9.3E-06 | 5.9E-06 | 5.6E-06 | 4.5E-07 | 4.0E-06 | 1.1E-04 |
| AM | 1.3E-04 | 5.5E-04 | 6.5E-04 | 1.1E-03 | 3.3E-04 | 1.3E-04 | 5.4E-05 | 5.6E-06 | 4.4E-05 | 3.0E-03 |
| AS | 1.8E-05 | 6.7E-05 | 7.8E-05 | 1.6E-04 | 3.5E-05 | 1.6E-05 | 7.0E-06 | 7.2E-07 | 6.6E-06 | 3.9E-04 |
| AT | 1.0E-04 | 1.7E-04 | 3.1E-04 | 2.0E-03 | 1.5E-04 | 2.0E-04 | 2.7E-04 | 3.2E-05 | 1.7E-04 | 3.4E-03 |
| AZ | 2.2E-06 | 7.7E-06 | 1.1E-05 | 2.2E-05 | 4.9E-06 | 2.2E-06 | 8.7E-07 | 8.5E-08 | 7.7E-07 | 5.1E-05 |
| BA | 2.2E-04 | 2.6E-04 | 4.7E-04 | 2.3E-03 | 3.2E-04 | 2.3E-04 | 2.1E-04 | 1.9E-05 | 1.4E-04 | 4.1E-03 |
| BE | 1.3E-04 | 2.2E-04 | 3.8E-04 | 3.1E-03 | 1.9E-04 | 1.9E-04 | 9.4E-04 | 8.6E-05 | 1.0E-03 | 6.3E-03 |
| BG | 2.7E-05 | 1.0E-04 | 1.3E-04 | 4.1E-04 | 7.5E-05 | 4.3E-05 | 3.3E-05 | 3.0E-06 | 3.2E-05 | 8.5E-04 |
| BY | 6.6E-05 | 9.8E-05 | 1.7E-04 | 7.8E-04 | 1.4E-04 | 1.5E-04 | 2.4E-05 | 4.2E-06 | 3.4E-05 | 1.5E-03 |
| CH | 5.1E-05 | 9.5E-05 | 1.6E-04 | 1.0E-03 | 7.2E-05 | 7.6E-05 | 2.2E-04 | 2.1E-05 | 1.8E-04 | 1.9E-03 |
| CY | 1.0E-07 | 5.7E-07 | 5.2E-07 | 7.1E-07 | 2.0E-07 | 9.6E-08 | 4.4E-08 | 4.7E-09 | 4.1E-08 | 2.3E-06 |
| CZ | 8.4E-04 | 9.9E-04 | 2.3E-03 | 2.1E-02 | 1.1E-03 | 1.6E-03 | 2.7E-03 | 3.3E-04 | 2.1E-03 | 3.3E-02 |
| ES | 8.0E-05 | 2.2E-04 | 2.5E-04 | 1.2E-03 | 1.1E-04 | 9.0E-05 | 3.3E-04 | 2.5E-05 | 2.6E-04 | 2.5E-03 |
| FR | 1.8E-04 | 3.6E-04 | 5.1E-04 | 3.4E-03 | 2.5E-04 | 2.2E-04 | 9.4E-04 | 8.5E-05 | 9.1E-04 | 6.9E-03 |
| GB | 5.7E-04 | 7.2E-04 | 1.5E-03 | 9.6E-03 | 8.9E-04 | 7.0E-04 | 3.2E-03 | 2.8E-04 | 2.6E-03 | 2.0E-02 |
| GE | 2.1E-06 | 9.4E-06 | 1.1E-05 | 1.8E-05 | 5.5E-06 | 2.2E-06 | 8.8E-07 | 9.0E-08 | 7.0E-07 | 5.0E-05 |
| GR | 2.5E-05 | 1.0E-04 | 1.4E-04 | 4.0E-04 | 6.9E-05 | 3.8E-05 | 4.3E-05 | 3.4E-06 | 3.3E-05 | 8.6E-04 |
| HR | 3.2E-05 | 4.0E-05 | 7.6E-05 | 3.7E-04 | 4.7E-05 | 4.3E-05 | 2.6E-05 | 2.5E-06 | 1.7E-05 | 6.5E-04 |
| HU | 1.6E-04 | 2.3E-04 | 4.4E-04 | 2.2E-03 | 2.1E-04 | 2.2E-04 | 1.7E-04 | 2.0E-05 | 1.0E-04 | 3.7E-03 |
| IE | 2.1E-05 | 3.4E-05 | 5.9E-05 | 3.1E-04 | 3.0E-05 | 2.2E-05 | 1.0E-04 | 9.2E-06 | 7.5E-05 | 6.6E-04 |
| IS | 2.0E-07 | 4.8E-07 | 6.5E-07 | 1.9E-06 | 3.4E-07 | 2.2E-07 | 4.2E-07 | 3.8E-08 | 2.7E-07 | 4.5E-06 |
| IT | 3.3E-04 | 4.1E-04 | 7.6E-04 | 3.9E-03 | 5.3E-04 | 4.0E-04 | 4.7E-04 | 4.4E-05 | 3.0E-04 | 7.1E-03 |
| KY | 1.3E-06 | 3.0E-06 | 4.8E-06 | 1.2E-05 | 2.4E-06 | 1.3E-06 | 4.0E-07 | 4.5E-08 | 3.8E-07 | 2.5E-05 |
| KZ | 1.6E-04 | 4.2E-04 | 6.5E-04 | 1.4E-03 | 3.3E-04 | 1.6E-04 | 5.4E-05 | 5.8E-06 | 5.1E-05 | 3.2E-03 |
| LI | 1.9E-08 | 3.5E-08 | 5.5E-08 | 3.7E-07 | 2.9E-08 | 3.2E-08 | 8.3E-08 | 7.6E-09 | 6.2E-08 | 7.0E-07 |
| LU | 4.4E-06 | 9.6E-06 | 1.3E-05 | 9.2E-05 | 6.4E-06 | 5.6E-06 | 2.6E-05 | 2.2E-06 | 2.8E-05 | 1.9E-04 |
| MC | 1.4E-07 | 2.3E-07 | 4.0E-07 | 1.5E-06 | 2.3E-07 | 1.6E-07 | 3.2E-07 | 2.6E-08 | 1.9E-07 | 3.2E-06 |
| MD | 8.9E-06 | 2.1E-05 | 2.6E-05 | 8.3E-05 | 1.9E-05 | 9.5E-06 | 4.5E-06 | 7.1E-07 | 7.0E-06 | 1.8E-04 |
| ME | 5.3E-06 | 8.2E-06 | 1.3E-05 | 6.4E-05 | 9.8E-06 | 6.0E-06 | 6.8E-06 | 6.3E-07 | 4.6E-06 | 1.2E-04 |
| MK | 8.8E-06 | 3.2E-05 | 4.3E-05 | 1.7E-04 | 2.5E-05 | 1.6E-05 | 2.0E-05 | 1.8E-06 | 1.6E-05 | 3.3E-04 |
| MT | 1.6E-07 | 6.7E-07 | 7.4E-07 | 2.6E-06 | 4.4E-07 | 3.0E-07 | 2.0E-07 | 1.5E-08 | 2.1E-07 | 5.4E-06 |
| NL | 8.0E-05 | 1.1E-04 | 2.2E-04 | 2.0E-03 | 1.2E-04 | 1.3E-04 | 5.7E-04 | 6.0E-05 | 7.0E-04 | 4.0E-03 |
| NO | 3.8E-05 | 7.1E-05 | 1.2E-04 | 3.0E-04 | 4.0E-05 | 2.6E-05 | 1.3E-04 | 5.9E-06 | 3.6E-05 | 7.7E-04 |
| PT | 1.2E-05 | 3.4E-05 | 3.9E-05 | 1.9E-04 | 1.7E-05 | 1.3E-05 | 4.4E-05 | 3.6E-06 | 3.5E-05 | 3.8E-04 |
| RO | 1.7E-04 | 3.2E-04 | 5.2E-04 | 1.8E-03 | 3.1E-04 | 1.7E-04 | 1.2E-04 | 1.4E-05 | 1.3E-04 | 3.6E-03 |
| RS | 3.3E-04 | 3.6E-04 | 7.2E-04 | 3.4E-03 | 4.5E-04 | 3.1E-04 | 3.0E-04 | 3.0E-05 | 2.1E-04 | 6.1E-03 |
| SI | 2.2E-05 | 3.0E-05 | 6.5E-05 | 3.3E-04 | 3.0E-05 | 3.6E-05 | 2.5E-05 | 2.8E-06 | 1.5E-05 | 5.6E-04 |
| SK | 2.4E-04 | 3.3E-04 | 6.9E-04 | 4.4E-03 | 3.4E-04 | 4.1E-04 | 3.4E-04 | 4.5E-05 | 2.1E-04 | 7.1E-03 |
| TJ | 7.2E-07 | 1.4E-06 | 2.5E-06 | 6.4E-06 | 1.1E-06 | 7.0E-07 | 1.9E-07 | 2.2E-08 | 1.7E-07 | 1.3E-05 |
| TM | 3.9E-06 | 1.0E-05 | 2.3E-05 | 4.2E-05 | 7.7E-06 | 4.2E-06 | 1.5E-06 | 1.3E-07 | 1.3E-06 | 9.4E-05 |
| TR | 1.5E-04 | 6.4E-04 | 6.8E-04 | 1.3E-03 | 4.5E-04 | 2.3E-04 | 7.1E-05 | 6.6E-06 | 5.9E-05 | 3.6E-03 |
| UA | 4.4E-04 | 9.1E-04 | 1.5E-03 | 3.5E-03 | 9.3E-04 | 6.3E-04 | 1.8E-04 | 1.9E-05 | 1.7E-04 | 8.3E-03 |
| UZ | 1.4E-05 | 2.9E-05 | 5.3E-05 | 1.4E-04 | 2.5E-05 | 1.4E-05 | 4.1E-06 | 4.5E-07 | 4.2E-06 | 2.8E-04 |
| NSR | 0.100 | 0.289 | 0.350 | 1.008 | 0.167 | 0.100 | 0.135 | 0.014 | 0.105 | 2.267 |
| EMEP | 0.005 | 0.008 | 0.014 | 0.073 | 0.008 | 0.007 | 0.012 | 0.001 | 0.010 | 0.137 |
| HELCOM | 0.013 | 0.025 | 0.033 | 0.221 | 0.043 | 0.018 | 0.029 | 0.004 | 0.033 | 0.419 |
| Total | 0.118 | 0.322 | 0.397 | 1.303 | 0.217 | 0.125 | 0.176 | 0.019 | 0.148 | 2.823 |

Metadata

Technical information

1. Source:

Meteorological Synthesizing Centre East (MSC-E) of EMEP.

2. Description of data:

Levels of atmospheric deposition of heavy metals over the Baltic Sea for the period from 1990 to 2018 were obtained using the latest version of GLEMOD model developed at EMEP/MSC-E (<http://en.msceast.org/index.php/j-stuff/glemos>). The latest available official emission data for the HELCOM countries have been used in the model computations. Emissions of cadmium and mercury for each year of this period were officially reported by most of the HELCOM countries. These data are available from the EMEP Centre on Emission Inventories and Projections (CEIP) (<http://www.ceip.at/>). The information on the heavy metal emission data used for modelling is presented in the indicator report on the HM emission to the air.

3. Geographical coverage:

Atmospheric deposition of cadmium and mercury were obtained for the European region and surrounding areas covered by the EMEP modelling domain.

4. Temporal coverage:

Time-series of annual atmospheric deposition are available for the period 1990 – 2018.

5. Methodology and frequency of data collection:

Atmospheric input and source allocation budgets of heavy metals (cadmium and mercury) to the Baltic Sea and its catchment area were computed using the latest version of GLEMOD model over the new EMEP domain (https://www.ceip.at/ms/ceip_home1/ceip_home/new_emep-grid/).

Global modelling framework GLEMOD is a multi-scale multi-pollutant simulation platform developed for operational and research applications within the EMEP programme [[Tarrason and Gusev, 2008](#); [Travnikov et al., 2009](#), [Jonson and Travnikov, 2010](#), [Travnikov and Jonson, 2011](#)]. The framework allows simulations of dispersion and cycling of different classes of pollutants (e.g. heavy metals and persistent organic pollutants) in the environment with a flexible choice of the simulation domain (from global to local scale) and spatial resolution. In the vertical the model domain covers the height up to 10 hPa (ca. 30 km). The current vertical structure consists of 20 irregular terrain-following sigma layers. Among them 10 layers cover the lowest 5 km of the troposphere and height of the lowest layer is about 75 m.

Anthropogenic emission data for modelling of cadmium and mercury have been prepared based on the gridded emissions fields provided by CEIP with spatial resolution 0.1x0.1 degree and complemented by additional emission parameters required for model runs. Data on wind re-suspension of Cd from soil and seawater has been generated using the dust pre-processor [[Gusev et al., 2006](#); [Ilyin et al., 2007](#)]. Atmospheric concentrations of chemical reactants and particulate matter, which are required for description of Hg chemistry, were imported from the MOZART and p-TOMCAT models [[Emmons et al., 2010](#); [Yang et al., 2005; 2010](#)]. Boundary conditions for the regional

scale simulations of all considered pollutants have been obtained from the GLEMOD model runs on a global scale.

Meteorological data used in the calculations for 1990-2018 were obtained using WRF meteorological data pre-processor [Skamarock *et al.*, 2008] on the basis of meteorological re-analyses data (ERA-Interim) of European Centre for Medium-Range Weather Forecasts (ECMWF).

Calculations of atmospheric transport and deposition of cadmium and mercury are provided on the regular basis annually two years in arrears on the basis of emission data officially submitted by the Parties to LRTAP Convention.

Normalized deposition values for the period 1990-2018 were obtained on the basis of results of model simulations using bi-exponential approximation [Colette *et al.*, 2016].

Quality information

6. Strength and weakness:

Strength: annually updated information on atmospheric input of cadmium and mercury to the Baltic Sea and its sub-basins.

Weakness: uncertainties in officially submitted emission data and secondary emissions of heavy metals.

7. Uncertainty:

Most of parameterizations of physical processes used in GLEMOD were transferred from previous model MSCE-HM used in operational modelling under EMEP [Travnikov and Ilyin, 2005]. The MSCE-HM model has been verified in a number of intercomparison campaigns with other regional HM transport models [Gusev *et al.*, 2000; Ryaboshapko *et al.*, 2001, 2005] and has been qualified by means of sensitivity and uncertainty studies [Travnikov, 2000]. It was concluded in these publications that the results of heavy metal airborne transport modelling were in satisfactory agreement with the available measurements and the discrepancies did not exceed on average a factor of two. The comparison of calculated versus measured data indicates that for most of stations in the Baltic region the deviation of annual modelled and observed concentrations in air and wet deposition fluxes of cadmium does not exceed a factor of two. Modelled wet deposition fluxes of mercury agree with the observed values within $\pm 50\%$ for most of stations. The agreement for annual mean concentrations of mercury in air is $\pm 10\%$.

The model was thoroughly reviewed at the workshop held in October, 2005 under supervision of the EMEP Task Force of Measurements and Modelling (TFMM). It was concluded that “MSC-E model is suitable for the evaluation of long-range transboundary transport and deposition of HMs in Europe” [ECE/EB.AIR/GE.1/2006/4].

8. Further work required:

Further work is required to reduce uncertainties in HM modelling approaches applied in the GLEMOD model.

References

- Colette et al. [2016]. Air pollution trends in the EMEP region between 1990 and 2012. EMEP: CCC-Report 1/2016. 105 p.
- Emmons L.K., Walters S., Hess P.G., Lamarque J.-F., Pfister G.G., Fillmore D., Granier C., Guenther A., Kinnison D., Laepple T., Orlando J., Tie X., Tyndall G., Wiedinmyer C., Baugcum S.L., and Kloster S. [2010] Description and evaluation of the Model for Ozone and Related chemical Tracers, version 4 (MOZART-4), Geosci. Model Dev., 3, 43–67, doi:10.5194/gmd-3-43-2010.
- Gauss M., Gusev A., Aas W., Klein H. and Nyiri A. [2019]. Atmospheric Supply of Nitrogen, Cadmium, Lead, Mercury, and PCDD/Fs to the Baltic Sea in 2017. Summary Report for HELCOM. MSC-W Technical Report 1/2019. <https://emeplint/publ/helcom/2019/index.html>
- Gauss M., A. Gusev, W. Aas [2020] Atmospheric Supply of Nitrogen, Cadmium, Lead, Mercury, PCDD/Fs, Benzo(a)pyrene and PCB-153 to the Baltic Sea. Summary Report for HELCOM. MSC-W Technical Report 1/2020.
- Gusev A., Ilyin I., Petersen G., van Pul A. and Syrakov D. [2000] Long-range transport model intercomparison studies. Model intercomparison study for cadmium. EMEP/ESC-E Report 2/2000, Meteorological Synthesizing Centre – East, Moscow, Russia. (http://www.msceast.org/reports/2_2000.pdf)
- Gusev A., Ilyin I., Mantseva L., Rozovskaya O., Shatalov V. and Travnikov O. [2006]. Progress in further development of MSCE-HM and MSCE-POP models (implementation of the model review recommendations). EMEP/MSC-E Technical Report 4/2006. 148 p.
- Ilyin I., Rozovskaya O., Sokovykh V. and Travnikov O. [2007]. Atmospheric modelling of heavy metal pollution in Europe: Further development and evaluation of the MSCE-HM model. EMEP/MSC-E Technical Report 4/2007. 58 p.
- Jonson J. E. and Travnikov O. (Eds.). [2010] Development of the EMEP global modeling framework: Progress report. Joint MSC-W/MSC-E Report. EMEP/MSC-E Technical Report 1/2010.
- Ryaboshapko A., Ilyin I., Bullock R., Ebinghaus R., Lohman K., Munthe J., Petersen G., Seigneur C., Wangberg I. [2001] Intercomparison study of numerical models for long-range atmospheric transport of mercury. Stage I: Comparison of chemical modules for mercury transformations in a cloud/fog environment. EMEP/MSC-E Technical report 2/2001, Meteorological Synthesizing Centre – East, Moscow, Russia. (http://www.msceast.org/reports/2_2001.pdf)
- Ryaboshapko A., Artz R., Bullock R., Christensen J., Cohen M., Draxler R., Ilyin I., Munthe J., Pacyna J., Petersen G., Syrakov D., and Travnikov O. [2005] Itercopmparison study of numerical models for long-range atmospheric transport of mercury. Stage III. Comparison of modelling results with long-term observations and comparison of calculated itens of regional balances. EMEP/MSC-E Technical Report 1/2005, Meteorological Synthesizing Centre – East, Moscow, Russia. (http://www.msceast.org/reports/1_2005.pdf)
- Tarrasón L. and Gusev A. [2008] Towards the development of a common EMEP global modeling framework. MSC-W Technical Report 1/2008
- Skamarock W.C., Klemp J.B., Dudhia J., Gill D.O., Barker D.M., Duda M.G., Huang X-Y., Wang W. and Powers J.G. [2008]. A Description of the Advanced Research WRF Version 3. NCAR/TN-475+STR NCAR technical note.
- Travnikov O. [2000] Uncertainty analysis of heavy metals long-range transport modelling. EMEP/MSC-E Technical note 9/2000, Meteorological Synthesizing Centre - East, Moscow, Russia. (http://www.msceast.org/reports/9_2000.pdf)
- Travnikov O., J.E. Jonson, A.S Andersen, M. Gauss, A. Gusev, O. Rozovskaya, D. Simpson, V. Sokovykh, S. Valiyaveetil and P. Wind [2009] Development of the EMEP global modelling framework: Progress report. Joint MSC-E/MSC-W Report.EMEP/MSC-E Technical Report 7/2009.
- Travnikov O. and Jonson J. E. (Eds.). [2011] Global scale modelling within EMEP: Progress report. EMEP/MSC-E Technical Report 1/2011
- Travnikov O. and Ilyin I. [2005] Regional Model MSCE-HM of Heavy Metal Transboundary Air Pollution in Europe. EMEP/MSC-E Technical Report 6/2005. (http://www.msceast.org/reports/6_2005.pdf)
- Yang, X., Cox, R., Warwick, N., Pyle, J., Carver, G., O'Connor,F., and Savage, N. [2005] Tropospheric bromine chemistry and its impacts on ozone: A model study, J. Geophys. Res., 110, D23311, doi:10.1029/2005JD006244.
- Yang, X., Pyle, J. A., Cox, R. A., Theys, N., and Van Roozendael, M. [2010] Snow-sourced bromine and its implications for polar tropospheric ozone, Atmos. Chem. Phys., 10, 7763–7773, doi:10.5194/acp-10-7763-2010.